IBRACON Structures and Materials Journal
Revista IBRACON de Estruturas e Materiais
ISSN 1983-4195 ismj.org

ORIGINAL ARTICLE

Probabilistic chloride diffusion modelling in cracked concrete structures by transient BEM formulation

Modelagem probabilística da difusão de cloreto em estruturas de concreto fissurado pela formulação transiente do MEC

Vinícius de Barros Souza[a]
Edson Denner Leonel[a]

[a]Universidade de São Paulo – USP, Escola de Engenharia de São Carlos, Departamento de Engenharia de Estruturas, São Carlos, SP, Brasil

Received 17 August 2021
Accepted 29 October 2021

Abstract: Reinforcement corrosion is a concern in the structural engineering domain, since it triggers several pathological manifestations, reducing the structural service life. Chloride diffusion has been considered one of main causes of reinforcements' corrosion in reinforced concrete. Corrosion starts when the chloride concentration at the reinforcements interface reaches the threshold content, leading to depassivation, whose assessment of its time of starts is a major challenge. This study applied the transient Boundary Element Method (BEM) approach for modelling chloride diffusion in concrete pores. The subregion BEM technique effectively represented the cracks inherent to the material domain, and environmental effects were also considered. Because of the inherent randomness of the problem, the service life was evaluated within the probabilistic context; therefore, Monte Carlo Simulation (MCS) assessed the probabilistic corrosion time initiation. Three applications demonstrated the accuracy and robustness of the model, in which the numerical results achieved by BEM were compared against numerical, analytical, and experimental responses from the literature. The probabilistic modelling substantially reduced the structural service life when the cracks length was longer than half of concrete cover thickness in highly aggressive environments.

Keywords: boundary element method, chloride diffusion, corrosion, structural durability, probabilistic analysis.

Resumo: A corrosão das armaduras é uma preocupação no domínio da engenharia estrutural, uma vez que este fenômeno desencadeia diversas manifestações patológicas, reduzindo a vida útil estrutural. A difusão do cloreto tem sido considerada uma das principais causas da corrosão das armaduras em concreto armado. A corrosão começa quando a concentração de cloreto na interface das armaduras atinge o teor limite, levando à despassivação, cuja avaliação do seu tempo de início é um grande desafio. Este estudo aplicou a abordagem transiente do Método dos Elementos de Contorno (MEC) para modelar a difusão de cloretos em poros do concreto. A técnica de sub-região do MEC possibilitou a representação de fissuras no domínio de forma eficaz, sendo também considerados efeitos ambientais. Por causa da inerente aleatoriedade do problema, a vida útil foi avaliada dentro do contexto probabilístico; portanto, a Simulação de Monte Carlo (SMC) avaliou o tempo de iniciação da corrosão probabilisticamente. Três aplicações demonstraram a precisão e robustez do modelo, no qual os resultados numéricos obtidos pelo MEC foram comparados com respostas numéricas, analíticas e experimentais da literatura. A modelagem probabilística reduziu substancialmente a vida útil estrutural quando o comprimento das fissuras superou a metade da espessura do cobrimento de concreto em ambientes altamente agressivos.

Palavras-chave: método dos elementos de contorno, difusão de cloreto, corrosão, durabilidade estrutural, análise probabilística.

How to cite: V. B. Souza and E. D. Leonel, "Probabilistic chloride diffusion modelling in cracked concrete structures by transient BEM formulation", *Rev. IBRACON Estrut. Mater.*, vol. 15, no. 4, e15402, 2022, https://doi.org/10.1590/S1983-41952022000400002

Corresponding author: Vinícius de Barros Souza. E-mail: vbarros@usp.br
Financial support: Coordenação de Aperfeiçoamento de Pessoal de Nível Superior - Brasil (CAPES) – Finance Code 001.
Conflict of interest: Nothing to declare.
Data Availability: The computational codes written in FORTRAN are stored in digital media and fully available in the "Laboratório de Informática e Mecânica Computacional do SET/EESC/USP". The authors share these files kindly on demand.

1 INTRODUCTION

Structural durability is a concern in the engineering domain, particularly in civil engineering, which largely employs reinforced concrete (RC) structures. The coupling of steel and concrete leads to effective structural systems and provides alternatives for magnificent architectural designs, chemical and thermal protection, and complementary mechanical behaviour. The service life concept frequently assesses the durability of RC structures and comprehends the time span for adequate material and structural performance [1]. Because RC is a porous-cracked composite material often exposed to environmental actions, the prediction of service life is a complex task and requires the development of robust and accurate frameworks despite the time span values suggested by design codes.

Pathological manifestations such as cover cracking, leaching, spalling, and reinforcement corrosion substantially reduce the durability of RC structures - the latter is the main mechanism, affecting approximately 58% of such structures and leading to 1% to 5% economic loss in the gross domestic product [2]–[5]. Chloride ingress is one of the main triggering causes of reinforcements corrosion, whose nature is often electrochemical in RC structures [6]. Chloride ions (Cl^-) penetrate the concrete pores by diffusion, and the reinforcements corrosion starts when the chloride concentration at the concrete/reinforcement interface reaches the threshold content [7], eliminating the passivation layer. Therefore, an accurate prediction of the time of corrosion initiation enables adequate assessments of structural durability.

The chloride diffusion process can be modelled by analytical approaches such as Fick's law [8]–[13]; however, analytical solutions account for inherent simplifications (e.g., time-independent boundary conditions, inert materials, body's geometry, material homogeneity, and dimensionality domain). Since structural materials in general do not satisfy such hypotheses, those approaches are non-robust for real-world applications.

On the other hand, numerical methods offer strategies for a proper modelling of the diffusion phenomenon. The Finite Element Method (FEM) and its extended version (XFEM) have been largely adopted for this purpose [14]–[21]; however, they both require domain mesh, which introduces domain approximations. Besides, an accurate assessment of domain variables leads to refined spatial and temporal discretisation, hence, a high number of degrees of freedom and large systems of algebraic equations [22]. These approaches may also lead to large computational time-consuming techniques, which make recursive or even parametric modelling prohibitive.

BEM effectively models the diffusion phenomenon and because this approach enables a boundary integral representation of the problem, the mesh required has a one-order dimensionality reduction. Moreover, discretisation is at the body's boundary and no domain mesh is needed. The latter aspect enables an accurate assessment of internal fields, which is attractive in diffusion problems with geometric details such as cracks, and relevant in durability assessments, which require a precise determination of the chloride concentration at the concrete/reinforcements interface. Discretisation solely at the boundary provides a solution with few degrees of freedom in comparison to domain methods. Therefore, BEM is adequate for parametric or even recursive analyses, as those required in probabilistic modelling [23]–[25].

Despite its accuracy, BEM has been marginally applied for solving corrosion time initiation and durability problems. Yang et al. [26], [27] adopted it for the diffusion modelling of chloride ions into cover thickness of concrete structures, and Chen et al. [28] analysed chloride diffusion in high-performance concretes, in which the BEM performance was compared against experimental results. Pellizzer and Leonel [29] modelled chloride ingress in concrete pores using the time-dependent BEM approach for diffusion, and later [30] proposed a Reliability-Based Design Optimisation (RBDO) formulation for the probabilistic optimisation of cover thickness in concrete structures subjected to chloride penetration. The present study contributes to the field applying the transient BEM approach for the time-dependent diffusion modelling of chlorides in concrete structures. The novelty involves the cracks influence modelling, which are preferential ingress paths. Such material discontinuities inherent to the concrete microstructure were discretely accounted, thus extending the state-of-the-art of the problem and enabling a realistic diffusion modelling in concrete pores.

Huge uncertainties influence the chloride diffusion processes and, since this phenomenon depends upon temperature, moisture, concrete mechanical integrity, structural loadings, concrete topology microstructure, among others, deterministic approaches fail in accurately predicting the chloride concentration and its evolution along time [31]–[33]. Consequently, the phenomenon can be handled solely in the probabilistic framework. For such purpose, First Order Reliability Method (FORM) or even Second Order Reliability Method (SORM) might be utilised; however, the inherent phenomenon complexities do not enable the process description by a single set of equations. The robust problem description requires numerical methods and implicit representations, as those adopted in this study. This aspect leads to numerical derivatives within FORM and SORM procedures, which may introduce a lack of convergence in several cases. Besides, the design point cannot be accurately determined in high nonlinear probabilistic problems, such as those handled herein, which make those solution techniques non-effective. Monte Carlo Simulation (MCS) is an adequate approach for assessing the probability of failure for the problems considered in this study. Since it requires a large range of simulations for an accurate probability of failure assessment, its

computation cost is a concern. Nevertheless, the computational effectiveness of BEM enables a probabilistic description via MCS. Very few studies have adopted this coupling scheme [29], [30], [34], thus motivating this research, which deals with the probabilistic modelling of chloride ingress in concrete pores.

The transient BEM formulation for diffusion handles the phenomenon description, whereas its coupling with MCS accounts for the uncertainties modelling. High-order boundary elements perform spatial approximations and the constant interpolation scheme approximates the temporal variables. BEM model accounts the presence of cracks and their influence upon the chloride flux velocity, which is the novelty in this study. Because concrete is cracked by loading and cure actions, the cracks representation enables an accurate and realistic problem modelling. Environmental effects such as chloride binding, temperature, and loadings were included in the modelling, which is a contribution of the study. Three applications demonstrated the accuracy and robustness of the proposed framework. The BEM results were compared against numerical, analytical, and experimental responses from the literature in applications one and two. The third application described the probabilistic modelling for tidal zones and highly aggressive environments.

2 TRANSIENT FORMULATION

2.1 Integral equations and BEM formulation

The following differential equation governs the transient diffusion problem (Equation 1):

$$\nabla^2 u - \frac{1}{k}\frac{\partial u}{\partial t} = 0 \tag{1}$$

where u represents the potential, t is time and k denotes the diffusion coefficient.

The solution of the differential equation requires boundary conditions regarding potential (u) and flux (q), as in Equations 2-3:

$$u(x,t) = \overline{u}(x,t) \; x \in \Gamma_1, \tag{2}$$

$$q(x,t) = \overline{q}(x,t) \; x \in \Gamma_2, \tag{3}$$

and initial conditions (Equation 4):

$$u(x,t_0) = u_0(x) \; x \in \Omega \tag{4}$$

where u_0 represents the potential conditions enforced along the domain (Ω) at the initial time (t_0), and $\overline{u}$ and $\overline{q}$ denote prescribed potential values in Γ_1 and prescribed flux values in Γ_2, respectively, where $\Gamma = \Gamma_1 \cup \Gamma_2$ is the body boundary. Flux is the directional derivative of u in relation to the outward normal vector to the boundary (η), i.e. $q = \partial u / \partial \eta$. In the present study, the potential represents the chloride concentration at a given point x for time t and q chloride flux.

Wrobel [35] demonstrated Equation 1 provides a boundary integral representation applying one of the following approaches: Laplace Transformation, Dual Reciprocity Method, or Time-Dependent Fundamental Solution. This study has adopted the latter; therefore, Green's second identity is applied to Equation 1 towards the boundary integral representation. The application of weighted residual technique, the integration of the resulting kernels by parts, and the classical limit process lead to the following integral equation:

$$c(\xi)u(\xi,t_F)+\int_{t_0}^{t_F}\int_{\Gamma}u(x,t)\ q^*(\xi,x,t_F,t)k\ d\Gamma\ dt=\int_{t_0}^{t_F}\int_{\Gamma}q(x,t)\ u^*(\xi,x,t_F,t)k\ d\Gamma\ dt+\int_{\Omega}u_0(x)\ q^*(\xi,x,t_F,t_0)k\ d\Omega \tag{5}$$

where x indicates the field points and ξ denotes the source points, t_0 is the initial time and t_F is the observation time, u^* and q^* are the time-dependent fundamental solutions to potential and flux, respectively, and c is the BEM free term. The free term value depends upon the source point position; it equals 0.5 for source point on smooth boundaries, such as those used here.

Equation 5 contains a domain integral, which can be transformed into a boundary integral by the Dual Reciprocity Method. Nevertheless, for the sake of simplicity, this term has been assumed nil, and Equation 5 can be rewritten as Equation 6.

$$c(\xi)u(\xi,t_F)+k\int_{t_0}^{t_F}\int_{\Gamma}u(x,t)\ q^*(\xi,x,t_F,t)d\Gamma\ dt=k\int_{t_0}^{t_F}\int_{\Gamma}q(x,t)\ u^*(\xi,x,t_F,t)d\Gamma\ dt. \tag{6}$$

For two-dimensional problems, the time-dependent fundamental solutions in Equation 6 are as follows (Equations 7-8) [35]:

$$u^*(\xi,x,t_F,t)=\frac{1}{4\pi k\tau}\exp\left(-\frac{r^2}{4k\tau}\right), \tag{7}$$

$$q^*(\xi,x,t_F,t)=-\frac{r\dfrac{\partial r}{\partial \eta}}{8\pi k^2\tau^2}\exp\left(-\frac{r^2}{4k\tau}\right), \tag{8}$$

where $\tau=t_F-t$ (t_F is analysis time), r indicates the distance between the source ξ and field x points, and $\dfrac{\partial r}{\partial \eta}=r_{,k}\,\eta_k$.

2.2 Algebraic representation

The numerical solution of Equation 6 requires spatial and temporal discretisation. Dividing boundary Γ into N_e boundary elements and time span t_F-t_0 into NT time steps, and inverting the order of integration in Equation 6, the following discretised equation can be obtained:

$$c_i\ u_i^{NT}=k\sum_{j=1}^{Ne}\sum_{n=1}^{NT}\int_{\Gamma_j}\int_{t_0^n}^{t_F^n}q^n\ u^*dt\ d\Gamma_j-k\sum_{j=1}^{Ne}\sum_{n=1}^{NT}\int_{\Gamma_j}\int_{t_0^n}^{t_F^n}u^n\ q^*dt\ d\Gamma_j \tag{9}$$

where u_i^{NT} is the potential value in source point i at time step NT, and t_0^n and t_F^n are initial and final times at time step n, respectively.

Equation 9 can be rewritten assuming a constant approximation along time and the positioning of collocation points at smooth boundaries. Therefore,

$$\sum_{n=1}^{NT}\sum_{j=1}^{Ne} H_{ij}^{n}\ u_{j}^{n} = \sum_{n=1}^{NT}\sum_{j=1}^{Ne} G_{ij}^{n}\ q_{j}^{n}, \tag{10}$$

where:

$$G_{ij}^{n} = k\int_{\Gamma_j} U_{n}^{*}\ d\Gamma_{\mathrm{j}}, \tag{11}$$

$$H_{ij}^{n} = \begin{cases} k\int_{\Gamma_j} Q_{n}^{*}\ d\Gamma_{j} + 0.5 \; if\ n = 1 \; and \; i = j, \\ \qquad k\int_{\Gamma_j} Q_{n}^{*}\ d\Gamma_{j} \; otherwise. \end{cases} \tag{12}$$

Equation 10 provides the algebraic system of equations for each boundary node. Therefore, the integration of U^{*} and Q^{*} leads to classical BEM influence matrices *G* and *H*, respectively. Because the problem is transient, the process solution requires a time-marching scheme [35], solved here as

$$\sum_{n=1}^{NT}\left[H\right]^{NT-n+1}\left\{u\right\}^{n} = \sum_{n=1}^{NT}\left[G\right]^{NT-n+1}\left\{q\right\}^{n}. \tag{13}$$

Since half of the quantities at the boundary are unknown, Equation 13 can be solved by

$$\left[A\right]\left\{x\right\}^{NT} = \left[B\right]\left\{y\right\}^{NT} + \sum_{n=1}^{NT-1}\left(\left[G\right]^{NT-n+1}\left\{q\right\}^{n} - \left[H\right]^{NT-n+1}\left\{u\right\}^{n}\right), \tag{14}$$

where $\left[A\right]$ and $\left[B\right]$ contain columns from *G* and *H* matrices evaluated at the first time step. More specifically, $\left[A\right]$ contains the influence terms associated with unknown variables, and $\left[B\right]$ contains the influence terms related to prescribed variables. Vectors $\left\{y\right\}^{NT}$ and $\left\{x\right\}^{NT}$ contain, respectively, the prescribed and unknown quantities at the boundary for the NT time step.

The singular kernels in Equations 11 and 12 were regularized by the semi-analytical method known as Singularity Subtraction Technique [36], whereas the non-singular ones were integrated by the Gauss-Legendre quadrature.

Equation 9 also assesses the chloride concentration at the domain. In such case, the free term equals unity since the collocation point is positioned at the domain. Thus, the chloride concentration can be evaluated by the following algebraic representation:

$$\left\{u_{i}\right\}^{NT} = \sum_{n=1}^{NT}\left(\sum_{j=1}^{Ne} G_{ij}^{'n}\ q_{j}^{n} - \sum_{j=1}^{Ne} H_{ij}^{'n}\ u_{j}^{n}\right), \tag{15}$$

where $G_{ij}^{'n} = k\int_{\Gamma_j} U_{n}^{*}\ d\Gamma_{\mathrm{j}}$ and $H_{ij}^{'n} = k\int_{\Gamma_j} Q_{n}^{*}\ d\Gamma_{j}$.

Equation 15 can be solved by the time-marching process previously addressed, providing the chloride concentration at internal points (u_{int}):

$$\{u_{int}\}^{NT} = \sum_{n=1}^{NT}\left([G]^{NT-n+1}\{q\}^{n} - [H]^{NT-n+1}\{u\}^{n}\right). \tag{16}$$

3 SUBREGION BEM TECHNIQUE

The transient BEM formulation enables the diffusion modelling of homogeneous domains, i.e., with a single diffusion coefficient. Nevertheless, the formulation represents the diffusion in non-homogeneous materials when coupled to the classical subregion BEM technique, which discretises the non-homogeneous domain into homogeneous piecewise regions where the compatibility of potentials and equilibrium of fluxes are enforced along the materials interfaces, as depicted in Figure 1.

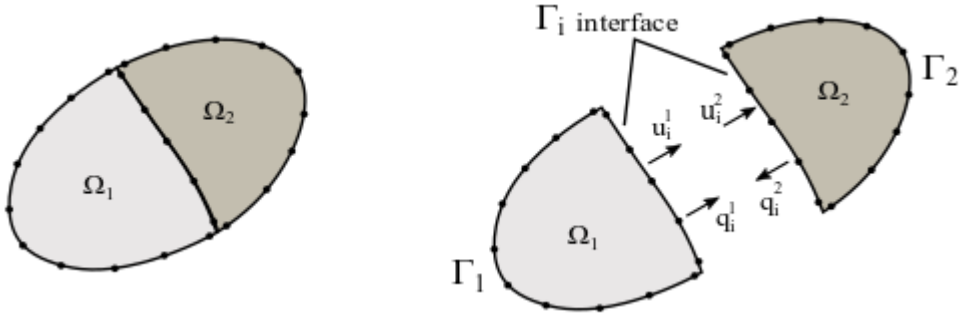

Figure 1. Discretisation in subregions and imposition of continuity on materials interfaces.

The algebraic operations required in the subregion BEM technique can be performed straightforwardly in a two-domain problem (Figure 1). In this case, Equations 11 and 12 lead to the following algebraic representation:

$$\begin{bmatrix} H^1 & H_i^1 & 0 & 0 \\ 0 & 0 & H^2 & H_i^2 \end{bmatrix} \begin{Bmatrix} u^1 \\ u_i^1 \\ u^2 \\ u_i^2 \end{Bmatrix} = \begin{bmatrix} G^1 & G_i^1 & 0 & 0 \\ 0 & 0 & G^2 & G_i^2 \end{bmatrix} \begin{Bmatrix} q^1 \\ q_i^1 \\ q^2 \\ q_i^2 \end{Bmatrix}, \tag{17}$$

where the superscript index indicates the domain and i denotes the material interface.

Since potentials and fluxes are indeterminate along the material interfaces, Equation 17 requires the following compatibility and equilibrium conditions for a proper solution (Equations 18-19):

$$u_i^1 = u_i^2, \tag{18}$$

$$q_i^1 = -q_i^2. \tag{19}$$

The coupling of Equations 17-19 leads to the following system:

$$\begin{bmatrix} H^1 & H_i^1 & 0 \\ 0 & H_i^2 & H^2 \end{bmatrix} \begin{Bmatrix} u^1 \\ u_i^1 \\ u^2 \end{Bmatrix} = \begin{bmatrix} G^1 & G_i^1 & 0 \\ 0 & -G_i^2 & G^2 \end{bmatrix} \begin{Bmatrix} q^1 \\ q_i^1 \\ q^2 \end{Bmatrix}. \tag{20}$$

Equation 20 can be solved by simply enforcing the boundary conditions, which triggers the classical columns change procedure of BEM. The subregion BEM technique provides generality to the numerical technique because non-homogeneous materials can be properly handled, and can also be applied for representing cracks. For such a purpose, the material interfaces contain the crack surfaces. Therefore, the entire domain requires a division into subregions, where the compatibility of potentials and equilibrium of fluxes must not be enforced along the crack surfaces, which become ordinary boundaries. The subregion approach does not require hypersingular integral equations, thus simplifying the integration process, and its application is straightforward when the kernels formulations are known.

4 DETERMINISTIC APPLICATIONS

4.1 Transient diffusion modelling in a square domain

A concrete column of square cross-section is exposed to an environment whose chloride ions (Cl^-) concentration is 1% of the concrete weight, as illustrated in Figure 2a. For the sake of simplicity, the problem symmetry properties were used. Therefore, a quarter of the domain was modelled and the symmetry boundary conditions assured the domain continuity (Figure 2b). The chloride diffusion coefficient is 10^{-12} m²/s (0.3154 cm²/year).

The application assesses the corrosion time initiation at the point depicted in Figure 2b, whose cover thickness is 5 cm for 20 years' structural lifetime. The analytical solution presented by Bitaraf and Mohammadi [13] and the numerical responses based on FEM, Finite Difference Method (FDM), Element-Free Galerkin (EFG), and Finite Point Method (FPM) are references herein and enable the verification of the BEM formulation accuracy.

The BEM mesh is composed of 40 isoparametric lagrangian elements with linear approximation, which leads to 44 collocation points (Figure 2c). The FPM modelling required a grid with 185 nodes, and the FEM employed 328 triangular elements with 185 nodes - the same number of nodes was used by the EFG method. The FDM results were provided by a 11x11 grid with 121 nodes [13], [37].

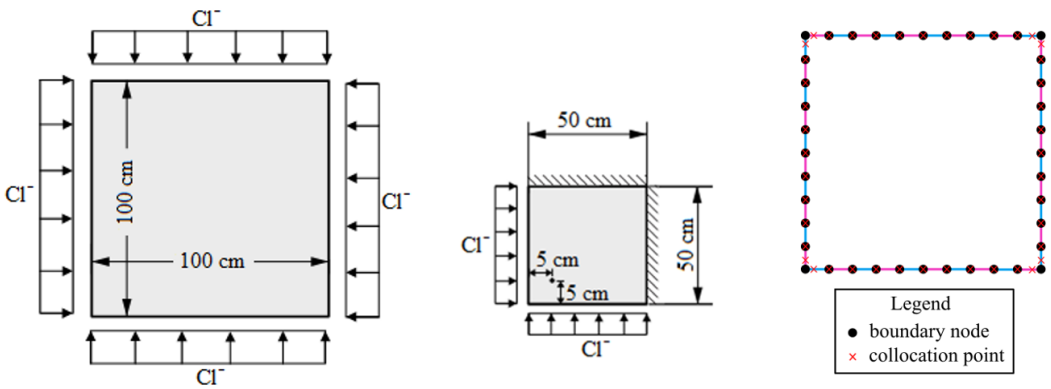

Figure 2. (a) Cross-section geometry and boundary conditions, (b) Symmetry boundary conditions, (c) BEM mesh.

The threshold chloride content for reinforcement depassivation is 0.10% of the concrete weight [13]. Figure 3 shows the results achieved by BEM, whose time was discretised within 20 time steps and the space kernels were integrated by 10 integration points, and the reference responses.

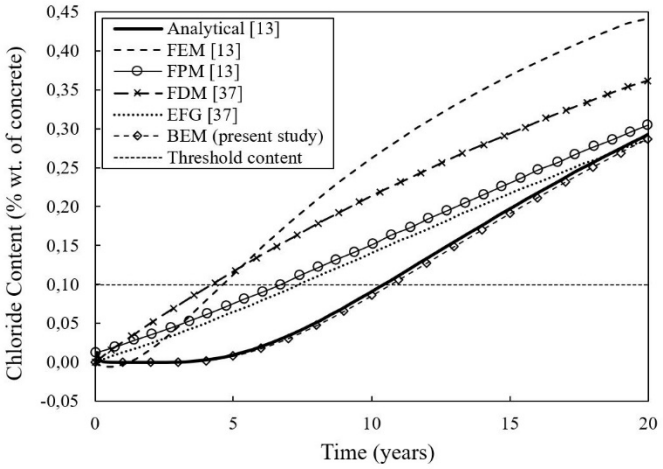

Figure 3. Chloride content evolution along time at 5 cm concrete cover.

The results in Figure 3 show the superior performance of BEM over other numerical approaches; its responses are in excellent agreement with the analytical predictions. BEM achieved such results with the coarsest mesh among the considered numerical methods, which demonstrates its accuracy.

BEM also accurately predicted the corrosion time initiation, i.e., the time span in which the chloride concentration at 5 cm cover is equal to the threshold content. The structural lifetime assessed by the analytical approach was 10.50 years. BEM predicted 10.65 years, showing a 1.4% difference in relation to the reference. The predictions of EFG, FPM, FEM, and FDM were, respectively, 7.58 years, 6.70 years, 4.67 years, and 4.33 years [13], highlighting the accuracy of BEM in diffusion modelling.

4.2 Diffusion modelling in a cracked material

The application deals with the chloride diffusion modelling in a cracked material. The responses provided by BEM were compared against the experimental results of Şahmaran [38], who conducted tests in prismatic specimens (355.6 x 50.8 x 76.2 mm) molded with mortar (w/c = 0.485) and reinforced with three levels of a 1 mm diameter steel reinforcement mesh in a 6 mm grid. After 43 days' curing in water, the specimens were pre-cracked using a 4-point bending test, which led to a single crack in the mortar samples. The unloaded specimens were immersed in a 3% NaCl solution for 30 days, after which their chloride concentration along the cracked area was quantified.

According to Şahmaran [38], the widths (w) of the cracks were narrower at a deeper level of the specimens than at the surface (V-shaped). An optical microscope measured such widths at five different points, providing a 29.4 μm average width and an 18.7 mm crack depth.

BEM used a two dimensional specimen of 356.0 mm x 76.0 mm cross-section for numerically reproducing the experiment. The crack was positioned at the cross-section centre and modelled by the subregion technique as a straight one parallel to the specimen's height (Figure 4a). The chloride content along the specimen's lower surface was 0.51% (per weight of cementitious materials), as suggested by Du et al. [39], who analysed the experimental data presented in [38]. The chloride concentration at the upper surface was nil, whereas the vertical surfaces were sealed with resin, leading to nil flux values. Therefore, such boundary conditions were enforced in the numerical modelling. The chloride diffusion coefficient in the mortar was $4.746x10^{-12}$ m^2/s (0.41 mm^2/day), considering ratio w/c = 0.485 [39].

Two subregions discretised the cross-section, requiring 150 isoparametric lagrangian elements of quadratic approximation and 320 nodes. The crack discretisation was composed of 7 nodes and positioned at the subregions interface. Figure 4b illustrates the boundary mesh.

Because of the capillarity effect along the crack surfaces, which appear due to their V-shape, the chloride concentration prescribed along the crack surfaces started with 0.51% at the crack mouth and reduced progressively at a 0.07% rate for each node, finishing with 0.09% at the crack tip. For the sake of simplicity, the reinforcements were not represented in the numerical model.

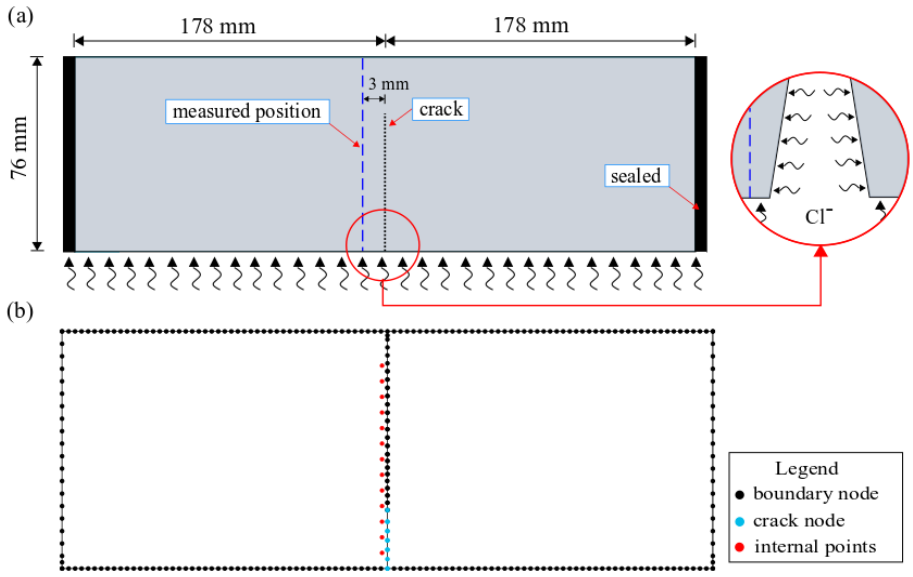

Figure 4. (a) Specimen geometry, (b) BEM mesh.

The red dots in Figure 4b represent the measuring points, which are equally spaced by 5 mm along the cross-section. The experimental analysis accounted for an uncracked specimen (w=0), which served as testimonial; the case was considered in the numerical modelling. The same BEM mesh was used in the testimonial modelling, in which both compatibility of chlorides concentration and equilibrium of fluxes were enforced along the crack nodes. Figure 5 displays the experimental results of Şahmaran [35] and the numerical responses achieved by BEM. The numerical modelling required 10 integration points for spatial integrations and 30 time steps in a 30-day time exposure to the NaCl solution.

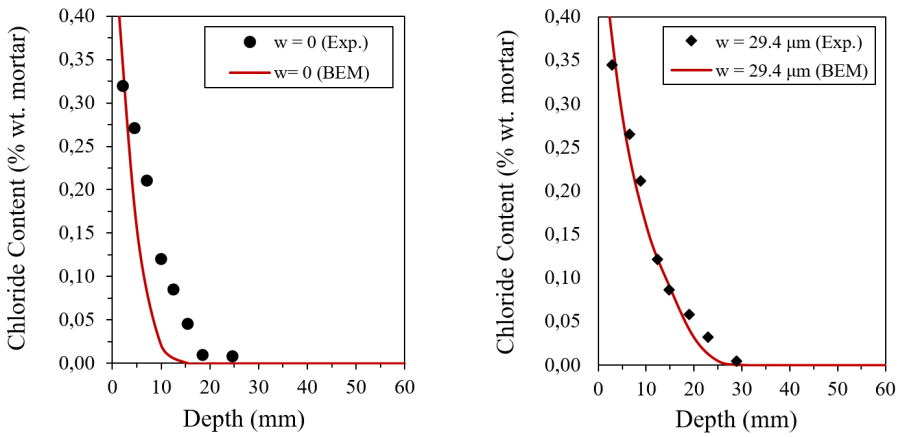

Figure 5. Comparison of results: Experimental (Exp.) [35] and numerical (BEM).

The numerical results provided by BEM are in good agreement with the experimental responses of Şahmaran [35] for the cracked specimen, although they underestimated the chloride concentration values for the $5 < \text{depth} < 15$ mm cover range in the non-cracked specimen. Nevertheless, the numerical modelling represented the crack influence on the chloride concentration distribution along the material domain, and the non-requirement of domain mesh by BEM provided high accuracy for the internal fields assessment.

5 PROBABILISTIC MODELLING: MONTE CARLO SIMULATION

Monte Carlo Simulation (MCS) is a numerical simulation technique developed by Metropolis and Ulam [40] that uses random numbers and limit state function simulations for uncertainty quantification purposes. In structural engineering applications, it usually assesses the probability of failure (P_f) of complex structures and structural systems subject to randomness. The probability of failure of a system can be determined by the integral of the joint probability density function (f_X) evaluated over the failure domain (Ω_f). However, the f_X function is implicit in complex engineering problems, hampering an explicit evaluation of the probability of failure, which can be assessed by simulation techniques that evaluate limit states punctually. In MCS, the simplest simulation technique, an indicator function $I[x]$ indicates if a simulated condition belongs to failure or safe conditions. The function is unitary when the simulated point belongs to the failure domain, and nil otherwise. Therefore, the probability of failure can be assessed by the following integral:

$$P_f = \int_{\Omega_f} f_X(x)\,dx = \int_{\Omega} I[x]\, f_X(x)\,dx\,. \tag{21}$$

Equation 21 can be estimated by a finite number of samples, n_s , according to:

$$P_f \approx \hat{P}_f = \frac{1}{n_s}\sum_{j=1}^{n_s} I\left[x_j\right] = \frac{n_f}{n_s}\,, \tag{22}$$

in which n_f is the number of samples in the failure domain and $\hat{P}_f$ is the estimated probability of failure.

Each evaluation of the indicator function involves a simulation of the limit state function, which defines the frontier between failure and safe domains. In the present study, the mechanic-probabilistic modelling is based on the limit state of corrosion initiation (G), defined by the difference between the threshold chloride content (C_{th}) and the chloride concentration (C) on the reinforcement interface, at point x and time t , as follows:

$$G(x,t) = C_{th} - C(x,t). \tag{23}$$

The chloride threshold has been often represented by deterministic values accounting for the class of environmental aggressiveness and concrete composition. Since the quantity displays an important randomness behaviour, C_{th} was modelled as a random variable in this study.

The probabilistic modelling performed here accounts for the environmental influence (e.g., temperature and chloride binding) on the concrete, as well as that of loads on the structure. Such effects were considered in the evaluation of the diffusion coefficient of concrete (k_0) by introducing penalization factors corresponding to chloride binding (F_1), temperature (F_2), and acting loads (F), as follows [41]:

$$k_0 = k_{\text{ref}}.F_1(C_b).F_2(T).F(\varepsilon,d), \tag{24}$$

where:

$k_{\text{ref}} =$ chloride diffusivity in saturated concrete at 28 days (m^2/s);

$C_b =$ bound chloride concentration (kg/m^3);

$T =$ reference temperature (K);

$\varepsilon =$ concrete compressive strain (‰);
$d =$ damage variable.

Diffusion coefficient k_{ref} is a parameter related to water cement ratio, *w/c*, and can be determined by the empirical expression proposed by Bentz et al. [42]:

$$k_{\text{ref}} = 10^{-10+4.66(w/c)}\ cm^2/s. \tag{25}$$

The factors in Equation 24 are detailed in Equations 26-29.

• Chloride binding factor

$$F_1(C_b) = \left[1 + \frac{\alpha}{\omega_e\left(1+\beta C_f\right)^2}\right]^{-1}, \tag{26}$$

where:
$\alpha, \beta =$ Langmuir constant values;
$\omega_e =$ evaporable water content;
$C_f =$ free chloride concentration (kg/m^3).

• Temperature factor

$$F_2(T) = \exp\left[\frac{U}{R}\left(\frac{1}{T_{\text{ref}}} - \frac{1}{T}\right)\right], \tag{27}$$

where:
$U =$ activation energy of the diffusion process (J. mol^{-1});
$R =$ gas constant (8.31 J. K^{-1}.mol^{-1});
$T_{\text{ref}} =$ current temperature (K).

• Acting loads factor

$$F(\varepsilon, d) = 1 + B\varepsilon + \frac{k_{\max}}{k_0}\left\{1 + C_1 d - \left[1 + \left(\frac{1}{d_{cr}}\right)^n\right]^{-1}\right\}, \tag{28}$$

where:
$B =$ parameter related to the concrete material irrespective of damage levels;
$k_{\max} =$ diffusion coefficient in completely damaged concrete (m^2/s);
$k_0 =$ diffusion coefficient in sound concrete (m^2/s);
$C_1, n, d_{\text{cr}} =$ model parameters.

When the concrete strain reaches the ultimate value (ε_u), damage variable d corresponds to 1 and the concrete is assumed completely damaged [41]. In this case, $C_1 = -Bk_s\varepsilon_u / k_{\max}$ and the loading factor can be simplified to Equation 29.

$$F\left(\varepsilon_u,1\right)=1+\frac{k_{\max}}{k_0}-\frac{k_{\max}}{k_0}\left[1+\left(\frac{1}{d_{cr}}\right)^n\right]^{-1}. \tag{29}$$

5.1. Probabilistic scenarios of chloride diffusion in a typical bridge beam

The application assesses the probability of reinforcement depassivation accounting for the influence of climatic conditions (temperature), chloride binding capacity, and effects of acting loads on an I shape cross-section commonly employed in bridge beams. It considers the beam a part of reinforced concrete structures exposed to tidal splashes.

The cross-sections largest dimensions are 90 cm x 40 cm, reinforced by eight 20 mm diameter rebars. Because of the high environmental aggressiveness, the concrete cover is 50 mm [43]. The beam connects the structural system by its upper boundary, which composes the structure deck; therefore, the chloride flux at this boundary is nil. The remaining cross-section boundaries, i.e., the lower and vertical are exposed to the chloride attack (Cl^-).

The subregion BEM technique represents the macrocracks in the numerical modelling. Their lengths are h and h $\sqrt{2}$, idealized as perfectly straight. For the sake of simplicity, the chloride concentration at the macrocrack surfaces equals that at the beam surface (C_0). Figure 6 illustrates the cross-section dimensions and macrocracks positions.

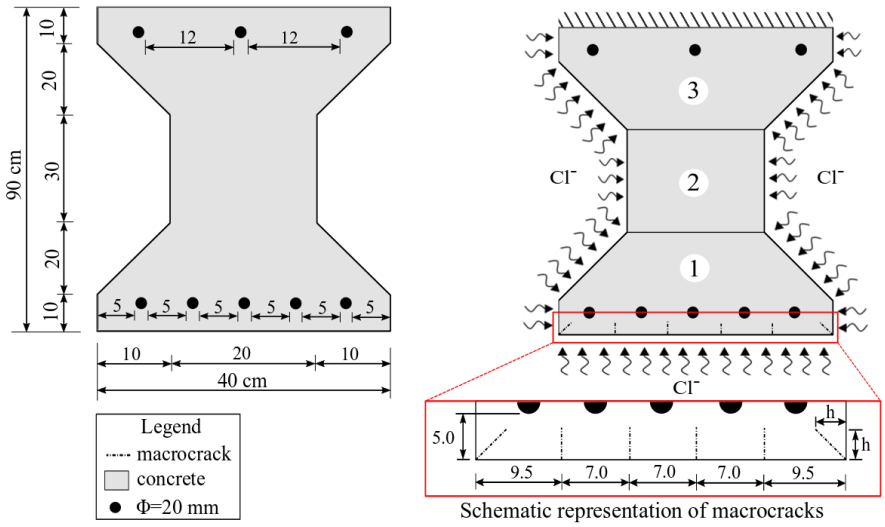

Figure 6. Cross-section geometry (measured in cm) and boundary conditions.

The cracks were positioned at the lower cross-section boundary towards representing the mechanical degradation in the concrete caused by tensile stress. The diffusion coefficient in region 1 accounts for the load factor (Equation 29); therefore, the analysed beam can be considered simply supported. The other effects (temperature and chloride binding) are equally considered in the diffusivity of regions 1, 2 and 3.

The probabilistic modelling accounts for three random variables. The *w/c* ratio data were adopted from Stewart et al. [44], who suggested 0.40 as the mean value for exposure to tidal or splash zones based on maximum *w/c* ratio specified in AS 5100.5. The coefficient of variation (C.O.V) assumed was 10% for concrete manufactured under controlled conditions, and the mean and C.O.V values of the surface chloride concentration (C_0) for splash zones were established by Val and Stewart [45], from data on offshore and onshore RC structures along the Australia coast reported by Collins and Grace [46] and McGee [47]. The chloride threshold content (C_{th}) was based on data provided by Vassie [48], who studied the percentage of corrosion cases in UK bridges in relation to the total chloride concentration at the reinforcement level [45]. Table 1 shows the input parameters of the model.

Table 1. Model input parameters.

Parameter	Mean	C.O.V	Distribution	Reference
C_0	7.35 kg/m^3	0.700	Lognormal	[45]
C_{th}	3.35 kg/m^3	0.375	Normal	[45]
w/c	0.40	0.040	Lognormal	-
C_f [1]	1.50 kg/m^3	-	Deterministic	[49]
U	44,600 J/mol	-	Deterministic	[50]
T_{ref}	296,15 K	-	Deterministic	[50]
T	300,30 K	-	Deterministic	-
$k_{\max} / k_0$ [2]	4.00	-	Deterministic	-

[1] Value correlated to $\omega_e = 0.6$, $\alpha = 11.8$ e $\beta = 4.0$ [49], [51]; [2] Model parameters: $n = 5$, $d_{cr} = 0.4$ [52].

The numerical modelling adopts the transient BEM approach, whose mesh at the external boundaries is composed of 172 isoparametric lagrangian elements of quadratic approximation, leading to 384 collocation points. Since the reinforcements are assumed non-porous media, the nil flux condition is enforced along their boundaries. Eight isoparametric boundary elements with quadratic approximation discretise each reinforcement boundary and 10 Gauss-Legendre points perform the space integrations, whereas 15 time steps discretise the analysis time.

Eight probabilistic scenarios enabled the assessment of isolated and joint influences of the environment and loadings on the chloride diffusion in concrete pores. Table 2 shows the scenarios considered, where dots indicate the presence of effect in the modelling. The even scenarios account for crack length with h=2 cm.

Table 2. Effects considered in each scenario.

Effect	Scenario							
	1	2	3	4	5	6	7	8
Chloride binding			•	•	•	•	•	•
Temperature					•	•	•	•
Acting load							•	•
Macrocracks		•		•		•		•

MCS performed the probabilistic simulations, in which 20,000 samples for each random variable describe safe and failure domains. Figure 7 shows the evolution of the probability of failure along time for a 75-year structural service-life.

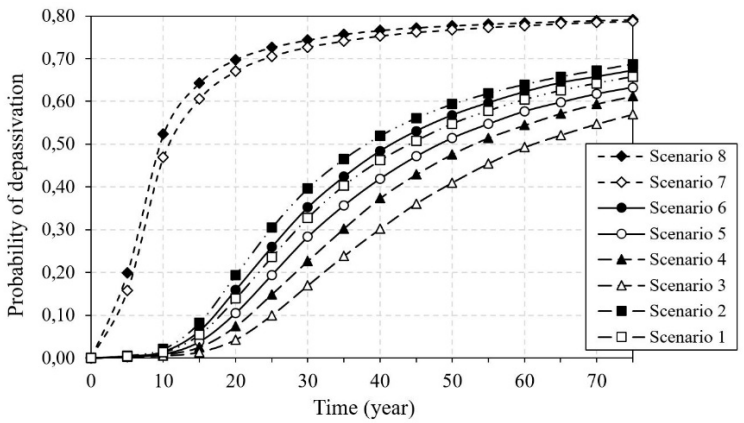

Figure 7. Probability of depassivation as a function of time for different scenarios.

Scenario 1, which disregards the influence of the effects, overestimates the probability of reinforcement depassivation when compared to scenarios that include the chloride binding capacity isolated and jointly with the influence of temperature or macrocracks on the concrete. At 50 years, the overestimation is 33%, 15%, and 6% for scenarios 3, 4, and 5, respectively, which is expected, since the effects of cracks and temperature accelerate the chloride diffusion, whereas chloride binding reduces the process, although in different proportions. The results also show the importance of representing environmental and mechanical influences on the diffusion process of chlorides in concrete for avoiding overestimation or underestimation of the design service life. Realistic frameworks such as those proposed here are fundamental for an accurate structural service life assessment.

The probability of failure significantly increases when the modelling accounts for the chloride binding capacity (see the curves for scenarios 1 and 3). This effect represents the concrete capacity for binding the free chlorides into its pores, and can be explained by the approximately 30% reduction in the F_1 factor (Equation 26). On the other hand, the temperature growth increases 28% the concrete diffusivity, whereas acting loads penalize this variable by 396%. Such environmental actions increase the probability of failure, as observed in scenario 5 in comparison to scenario 3, and scenario 7 in comparison to scenarios 3 and 5. The loading effects influenced the diffusion phenomenon more strongly than the temperature in the simulations, since the damage was complete. Nevertheless, different behaviours can be displayed if usual structural service loads are considered.

The loading effects assume a major importance in the diffusion modelling (see Figure 7), since they uniformly penalize the concrete diffusivity along the cross-section domain. However, cracks also increase the chloride diffusion velocity. Because their discontinuities introduce preferential ingress paths, the probability of failure increases when cracks are considered. The presence of 2 cm long cracks reduces 20% of the probabilistic structural service, which demonstrates their importance in the modelling.

The cracks influence can be further investigated. For this purpose, scenario 5 (h=0) are compared against scenario 6, in which the probabilistic modelling accounts for crack lengths increasing progressively with $1 \leq h \leq 4$ cm. Figure 8 displays the numerical responses provided by the transient BEM approach.

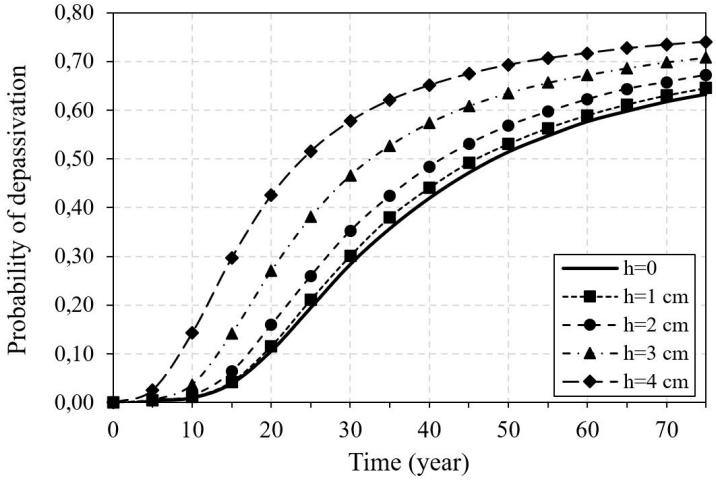

Figure 8. Influence of crack length on the probability of reinforcement depassivation.

The numerical results in Figure 8 show cracks with h equals 1 cm and 2 cm exert a small influence on the evolution of the probability of failure. However, the probability of failure significantly increases when h assumes 3 cm and 4 cm, which are higher than half of the cover thickness. Obviously, this behaviour accounts for severe environmental aggressiveness and 5 cm cover thickness. For 50-year time span, the probability of failure for 4 cm long crack is 35% higher than the case in which cracks are disregarded. Fib Bulletin 34 [53] recommends an 10% maximum depassivation probability for exposition to seawater. In such a context, the avoidance of cracks would extend the structural service life by 10 years, on average.

5 CONCLUSIONS

This study applied the transient BEM formulation for the chloride diffusion modelling in concrete pores. The approach was coupled to MCS for a probabilistic assessment of the structural service life, thus enabling a probabilistic assessment of durability in RC structures. Tidal zones were considered for an environmental aggressiveness description, and the numerical responses have led to the following conclusions:

1. BEM provided accurate results in comparison to other numerical techniques, such as FEM, EFG, FDM, and FPM, achieving superior performance with fewer degrees of freedom, which is an advantage when repetitive analyses are required, as in MCS.

2. The environment is fundamental in diffusion modelling. The chloride binding effect reduces the concrete diffusivity and, consequently, extends the structural service life by binding the free chlorides in the concrete pores. However, temperature and loading effects increase diffusivity and reduce structural durability, which is a concern, especially regarding global warming, since temperatures are expected to rise in the near future. Therefore, an accurate structural durability modelling must consider such effects.

3. The structural service life can be considerably reduced by cracks. Because cracks enable a preferential chloride ingress path, their length play a major role in the problem. The application considered herein suggests cracks length longer than half of the concrete cover thickness significantly reduces the probabilistic service life.

The model proposed herein is general and, for the sake of completeness, the authors adopted data from the literature for the applications. Nevertheless, the model can be applied for any geographical region if the required data are available.

ACKNOWLEDGEMENTS

The authors acknowledge Universidade de São Paulo (EESC/USP/Brazil) for their support and the research grant financed by Coordenação de Aperfeiçoamento de Pessoal de Nível Superior – Brasil (CAPES) – Finance Code 001.

REFERENCES

[1] E. Possan, “Modelagem da carbonatação e previsão de vida útil de estruturas de concreto em ambiente urbano,” Ph.D. dissertation, UFRGS, Porto Alegre, 2010.

[2] A. A. Nince and J. C. T. S. Clímaco “Levantamento de dados sobre deterioração de estruturas na Região Centro-Oeste do Brasil,” *Anais do Congress on High-Performance and Quality of Concrete Structures,* Florianópolis, SC, 1996.

[3] O. T. Rincón, A. R. Carruyo, C. Andrade, P. R. L. Helene, and I. Díaz, *Manual de Inspección, Evaluación y Diagnóstico de Corrosión en Estructuras de Hormigón Armado.* Rio de Janeiro: Iberoam Program Sci. Technol. Dev., 1998.

[4] M. Grochoski and P. R. L. Helene, *Sistemas de Reparo para Estruturas e Concreto com Corrosão de Armaduras* (USP Polytechnic School Technical Bulletin), São Paulo: USP, 2008, pp. 1–23.

[5] Grandes Construções, “Brasil perde 4% do PIB com corrosão,” *Aço na Construção*, May 17, 2017. [Online]. Available: https://www.grandesconstrucoes.com.br/Materias/Exibir/brasil-perde-4-do-pib-com-corrosao

[6] V. Gentil, *Corrosão*, 3th ed. Rio de Janeiro: Livros Técnicos e Científicos, 1996.

[7] K. Tuutti, "Service life of structures with regard to corrosion of embedded steel," *Spec. Publ.*, vol. 65, pp. 223–236, 1980.

[8] L. Collepardi, A. Marcialis, and R. Turriziani, "La cinetica di penetrazione degli ioni cloruro nel calcestruzzo," *Cemento*, vol. 67, no. 4, pp. 157–164, 1970.

[9] P. S. Mangat and B. T. Molloy, "Prediction of long term chloride concentration in concrete," *Mater. Struct.*, vol. 27, no. 6, pp. 338–346, 1994., http://dx.doi.org/10.1007/BF02473426.

[10] L. Mejlbro, “The complete solution of Fick’s second law of diffusion with time-dependent diffusion coefficient and surface concentration,” in *Durability Concr. Saline Environ.*, Lund, Sweden, 1996, pp. 127–158.

[11] M. K. Kassir and M. Ghosn, "Chloride-induced corrosion of reinforced concrete bridge decks," *Cement Concr. Res.*, vol. 2, no. 1, pp. 139–143, 2002, http://dx.doi.org/10.1016/S0008-8846(01)00644-5.

[12] M. Bitaraf and S. Mohammadi, "Analysis of chloride diffusion in concrete structures for prediction of initiation time of corrosion using a new meshless approach," *Constr. Build. Mater.*, vol. 22, no. 4, pp. 546–556, 2008, http://dx.doi.org/10.1016/j.conbuildmat.2006.11.005.

[13] S. Zhou, "Analytical model for square root increase of surface chloride concentration and decrease of chloride diffusivity," *J. Mater. Civ. Eng.*, vol. 28, no. 4, pp. 04015181, 2016, http://dx.doi.org/10.1061/(ASCE)MT.1943-5533.0001483.

[14] Y. Zeng, "Modeling of chloride diffusion in hetero-structured concretes by finite element method," *Cement Concr. Compos.*, vol. 29, no. 7, pp. 559–565, 2007, http://dx.doi.org/10.1016/j.cemconcomp.2007.04.003.

[15] C. Fu, X. Jin, and N. Jin, “Modeling of chloride ions diffusion in cracked concrete,” in *Earth and Space 2010: Eng. Sci. Constr. Oper. Challenging Environ.*, Honolulu, Hawaii, 2010, pp. 3579–3589, http://dx.doi.org/10.1061/41096(366)343.

[16] J. Xiao, J. Ying, and L. Shen, "FEM simulation of chloride diffusion in modeled recycled aggregate concrete," *Constr. Build. Mater.*, vol. 29, pp. 12–23, 2012, http://dx.doi.org/10.1016/j.conbuildmat.2011.08.073.

[17] R. Duddu, "Numerical modeling of corrosion pit propagation using the combined extended finite element and level set method," *Comput. Mech.*, vol. 54, no. 3, pp. 613–627, 2014, http://dx.doi.org/10.1007/s00466-014-1010-8.

[18] X.-Y. Wang and L.-N. Zhang, "Simulation of Chloride Diffusion in Cracked Concrete with Different Crack Patterns," *Adv. Mater. Sci. Eng.*, vol. 2016, pp. 1075452, 2016, http://dx.doi.org/10.1155/2016/1075452.

[19] H. S. Al-Alaily, A. A. A. Hassan, and A. A. Hussein, "Use of extended finite element method and statistical analysis for modelling the corrosion-induced cracking in reinforced concrete containing metakaolin," *Can. J. Civ. Eng.*, vol. 45, no. 3, pp. 167–178, 2018, http://dx.doi.org/10.1139/cjce-2017-0298.

[20] Y. Wu and J. Xiao, "The multiscale spectral stochastic finite element method for chloride diffusion in recycled aggregate concrete," *Int. J. Comput. Methods*, vol. 15, no. 1, pp. 1750078, 2018, http://dx.doi.org/10.1142/S0219876217500785.

[21] J. Peng, S. Hu, J. Zhang, C. S. Cai, and L. Li, "Influence of cracks on chloride diffusivity in concrete: a five-phase mesoscale model approach," *Constr. Build. Mater. Elsevier*, vol. 197, pp. 587–596, 2019, http://dx.doi.org/10.1016/j.conbuildmat.2018.11.208.

[22] L. F. Yang, Z. Chen, Q. Gao, and J. W. Ju, "Compensation length of two-dimensional chloride diffusion in concrete using a boundary element model," *Acta Mech.*, vol. 224, no. 1, pp. 123–137, 2013, http://dx.doi.org/10.1007/s00707-012-0721-1.

[23] L. C. Wrobel and D. B. Figueiredo, "Numerical analysis of convection-diffusion problems using the boundary element method," *Int. J. Numer. Methods Heat Fluid Flow*, vol. 1, no. 1, pp. 3–18, 1991, http://dx.doi.org/10.1108/eb017470.

[24] G. F. Dargush and P. K. Banerjee, "Application of the boundary element method to transient heat conduction," *Int. J. Numer. Methods Eng.*, vol. 31, no. 6, pp. 1231–1247, 1991, http://dx.doi.org/10.1002/nme.1620310613.

[25] E. D. Leonel, A. Chateauneuf, W. S. Venturini, and P. Bressolette, "Coupled reliability and boundary element model for probabilistic fatigue life assessment in mixed mode crack propagation," *Int. J. Fatigue*, vol. 32, no. 11, pp. 1823–1834, 2010, http://dx.doi.org/10.1016/j.ijfatigue.2010.05.001.

[26] L. F. Yang et al., "Analysis of chloride diffusion in concrete by the boundary element method," *J. Concr.*, pp. 25–28, 2008.

[27] L. F. Yang, Z. Chen, Y. Wang, W. Meng, L. Song, and Q. Feng, "Boundary element method for analysis of two-dimensional chloride diffusion in concrete," *J. Chin. Ceram. Soc.*, vol. 7, pp. 1110–1117, 2009.

[28] Z. Chen et al., "Analysis of chloride diffusion in high-performance concrete and its service life by the boundary element method," *J. Build. Mater*, vol. 13, pp. 97–103, 2010.

[29] G. P. Pellizzer and E. D. Leonel, "Probabilistic corrosion time initiation modelling in reinforced concrete structures using the BEM," *Rev. IBRACON Estrut. Mater.*, vol. 13, no. 4, e13409, 2020, http://dx.doi.org/10.1590/s1983-41952020000400009.

[30] G. P. Pellizzer and E. D. Leonel, "The cover thickness design of concrete structures subjected to chloride ingress from RBDO solution technique," *Rev. IBRACON Estrut. Mater.*, vol. 13, no. 5, e13502, 2020, http://dx.doi.org/10.1590/s1983-41952020000500002.

[31] D. V. Val and P. A. Trapper, "Probabilistic evaluation of initiation time of chloride-induced corrosion," *Reliab. Eng. Syst. Saf.*, vol. 93, no. 3, pp. 364–372, 2008, http://dx.doi.org/10.1016/j.ress.2006.12.010.

[32] B. Saassouh and Z. Lounis, "Probabilistic modeling of chloride-induced corrosion in concrete structures using first-and second-order reliability methods," *Cement Concr. Compos.*, vol. 34, no. 9, pp. 1082–1093, 2012, http://dx.doi.org/10.1016/j.cemconcomp.2012.05.001.

[33] U. M. Angst, "Predicting the time to corrosion initiation in reinforced concrete structures exposed to chlorides," *Cement Concr. Res.*, vol. 115, pp. 559–567, 2019, http://dx.doi.org/10.1016/j.cemconres.2018.08.007.

[34] Q. M. Jiang, L. F. Yang, and Z. Chen, "Stochastic analysis of chloride profiles in concrete structures," *Adv. Mat. Res.*, vol. 163-167, pp. 3364–3368, 2010, http://dx.doi.org/10.4028/www.scientific.net/AMR.163-167.3364.

[35] L. C. Wrobel, *The Boundary Element Method – Applications in Thermo-Fluids and Acoustics, vol. 1.* United Kingdom: John Wiley & Sons, 2002.

[36] M. Guiggiani and P. Casalini, "Direct computation of Cauchy principal value integrals in advanced boundary elements," *Int. J. Numer. Methods Eng.*, vol. 24, no. 9, pp. 1711–1720, 1987, http://dx.doi.org/10.1002/nme.1620240908.

[37] A. Farahani and H. Taghaddos, "Prediction of service life in concrete structures based on diffusion model in a marine environment using mesh free, FEM and FDM approaches," *J. Rehabil. Civ. Eng.*, vol. 8, no. 4, pp. 1–14, 2020., http://dx.doi.org/10.22075/jrce.2020.19189.1380.

[38] M. Şahmaran, "Effect of flexure induced transverse crack and self-healing on chloride diffusivity of reinforced mortar," *J. Mater. Sci.*, vol. 42, no. 22, pp. 9131–9136, 2007, http://dx.doi.org/10.1007/s10853-007-1932-z.

[39] X. Du, L. Jin, R. Zhang, and Y. Li, "Effect of cracks on concrete diffusivity: a meso-scale numerical study," *Ocean Eng. Elsevier*, vol. 108, pp. 539–551, 2015, http://dx.doi.org/10.1016/j.oceaneng.2015.08.054.

[40] N. Metropolis and S. Ulam, "The Monte Carlo method," *J. Am. Stat. Assoc.*, vol. 44, no. 247, pp. 335–341, 1949.

[41] C. Fu, X. Jin, H. Ye, and N. Jin, "Theoretical and experimental investigation of loading effects on chloride diffusion in saturated concrete," *J. Adv. Concr. Technol.*, vol. 13, no. 1, pp. 30–43, 2015, http://dx.doi.org/10.3151/jact.13.30.

[42] D. P. Bentz, J. R. Clifton, and K. A. Snyder, "Predicting service life of chloride-exposed reinforced concrete," *Concr. Int.*, vol. 18, no. 12, pp. 42–47, 1996.

[43] Associação Brasileira de Normas Técnicas, *Projeto de Estruturas de Concreto – Procedimento*, ABNT NBR 6118:2014, 2014.

[44] M. G. Stewart, X. Wang, and M. N. Nguyen, "Climate change impact and risks of concrete infrastructure deterioration," *Eng. Struct.*, vol. 33, no. 4, pp. 1326–1337, 2011, http://dx.doi.org/10.1016/j.engstruct.2011.01.010.

[45] D. V. Val and M. G. Stewart, "Life-cycle cost analysis of reinforced concrete structures in marine environments," *Struct. Saf.*, vol. 25, no. 4, pp. 343–362, 2003, http://dx.doi.org/10.1016/S0167-4730(03)00014-6.

[46] F. G. Collins and W. R. Grace, "Specifications and testing for corrosion durability of marine concrete: the Australian perspective," *Spec. Publ.*, vol. 170, pp. 757–776, 1997.

[47] R. McGee, "Modelling of durability performance of tasmanian bridges," in *ICASP8 Appl. Stat. Probab. Civ. Eng., vol. 1*, R. E. Melchers and M. G. Stewart, Eds., Rotterdam: Balkema, pp. 297–306, 1999.

[48] P. R. Vassie, "Reinforcement corrosion and the durability of concrete bridges," *Proc. Inst. Civ. Eng. Part 1*, vol. 76, no. 8, pp. 713–723, 1984, http://dx.doi.org/10.1680/iicep.1984.1207.

[49] E. Zacchei and C. G. Nogueira, "Chloride diffusion assessment in RC structures considering the stress-strain state effects and crack width influences," *Constr. Build. Mater.*, vol. 201, pp. 100–109, 2019, http://dx.doi.org/10.1016/j.conbuildmat.2018.12.166.

[50] D. Vieira, A. Moreira, J. Calmon, and W. Dominicini, "Service life modeling of a bridge in a tropical marine environment for durable design," *Constr. Build. Mater. Elsevier*, vol. 163, pp. 315–325, 2018, http://dx.doi.org/10.1016/j.conbuildmat.2017.12.080.

[51] T. Ishida, P. Iqbal, and H. Anh, "Modeling of chloride diffusivity coupled with non-linear binding capacity in sound and cracked concrete," *Cement Concr. Res. Elsevier*, vol. 39, no. 10, pp. 913–923, 2009, http://dx.doi.org/10.1016/j.cemconres.2009.07.014.

[52] B. Gerard, G. Pijaudier-Cabot, and C. Laborderie, "Coupled diffusion-damage modelling and the implications on failure due to strain localization," *Int. J. Solids Struct.*, vol. 35, no. 31–32, pp. 4107–4120, 1998, http://dx.doi.org/10.1016/S0020-7683(97)00304-1.

[53] Fédération Internationale Du Béton, *Model Code for Service Life Design*, FIB Bulletin 34:2006, 2006.

Author contributions: VBS: conceptualization, literature review, methodology, computational implementation & validation, formal analysis, written, illustration and editing. EDL: conceptualization, literature review, methodology, formal analysis, supervision, layout, writing-review.

Editors: Bruno Briseghella, Guilherme Aris Parsekian.